The Sensitivity of an Energy Balance Climate Model to Variations in the Orbital Parameters

Max J. Suarez

Department of Atmospheric Sciences, University of California, Los Angeles, California 90024

Isaac M. Held[1]

Center for Earth and Planetary Physics, Harvard University, Cambridge, Massachusetts 02138

The responses of a zonally symmetric model of the global energy balance to perturbations in incident solar radiation are analyzed. The model is forced with seasonally varying insolation and incorporates in a simple way the positive feedback due to the high albedo of snow and sea ice. Meridional energy transport due to atmospheric motions is simulated with lateral diffusion of heat. Meridional energy transport by oceanic currents is ignored, as are possible variations in cloudiness. Emphasis is placed on the model's sensitivity to the latitudinal and seasonal redistribution of insolation produced by variations in the obliquity, the eccentricity, and the longitude of perihelion of the earth's orbit. It is found that when albedos are allowed to vary, increased seasonal variation of insolation leads to increased temperature in the northern hemisphere. In all cases considered, the latitudinal extent of perennial snow cover in the northern hemisphere is particularly sensitive to the perturbations, a response suggestive of the large fluctuations of continental glaciers during the Pleistocene. When the model is forced with the orbital variations of the past 150,000 years, its response is qualitatively similar to the geologic record of that period.

1. Introduction

Recent analyses of paleoclimatic time series obtained from deep-sea cores [*Hays et. al.*, 1976] provide new evidence for the 'astronomical' or Milankovitch theory of the ice ages. Spectral analyses of these time series yield significant peaks at just those frequencies at which the earth's orbitral parameters are known to vary. This result is, we believe, of fundamental importance for our understanding of climatic sensitivity. If the climatic responses to these perturbations are indeed observable in paleoclimatic time series, we have a unique record of responses to known changes in external parameters against which to test theories of climatic sensitivity.

The most common criticism of the astronomical theory has been that the climatic responses to be expected from orbital parameter variations are much too small to explain the glacial-interglacial fluctuations of the Pleistocene [*Flint*, 1971]. However, recent work with various paleoclimate indicators, such as that done under the Climap project [*McIntyre et al.*, 1976], indicates that temperature differences between the last glacial maximum and the present climate are not as large as had earlier been thought. Differences in ocean surface temperature equatorward of 40° latitude average ~2°C, and larger temperature changes are primarily confined to high northern latitudes.

In addition, energy balance models of the earth's climate, which attempt to take into account surface albedo variations due to changing ice and snow cover, predict that these changes can produce a strong positive feedback to changes in insolation. There is at present no consensus on the quantitative importance of this effect, but the possibility exists, at least, that surface temperatures, particularly in high latitudes, are remarkably sensitive to changes in insolation.

Furthermore, perturbations in incident radiation resulting

from the orbital variations can be quite large at a given latitude and time of year (as we shall see in detail below), although there is admittedly considerable compensation when one averages over the year or over the globe. If climatic variables of interest can be shown to depend not just on annual or global mean insolation, but on the seasonal distribution of insolation as well, then one can hope to obtain substantial climatic responses from these perturbations.

Encouraged by these observations, we have examined the response to orbital parameter variations of a model of the earth's energy balance forced with seasonally varying insolation. The model uses a crude scheme to predict albedos as a function of latitude and time of year. The key to the model's responses is, in fact, the coupling between these seasonally varying albedos and the seasonally varying insolation. Briefly stated, we find that large obliquity and perihelion near northern hemisphere summer solstice produce the warmest climate. We find, in addition, that the northern hemisphere's perennial snow line over land, which we associate with the limit of continental glaciers, is an exceptionally sensitive part of the model.

2. The Orbital Parameters

The three orbital parameters of concern are the obliquity, the eccentricity, and the 'longitude of the perihelion.' The obliquity Φ is the angle between the axis of rotation and the normal to the orbital plane. It varies from ~22° to ~24.5° with a dominant period of 40,000 years. A larger obliquity results in a smaller meridional gradient in annual mean insolation and a larger seasonal variation. The eccentricity ϵ, defined as $[1 - (b/a)^2]^{1/2}$, where a and b are the semimajor and semiminor axes of the orbital ellipse, varies from ~0 to ~0.04, with a characteristic period of ~100,000 years. The semimajor axis (and therefore the period of revolution) remains unchanged. For an eccentric orbit the insolation also depends on the position of the perihelion with respect to the equinoxes. We define Π to be the angle between lines connecting the sun with the positions of perihelion and northern hemisphere au-
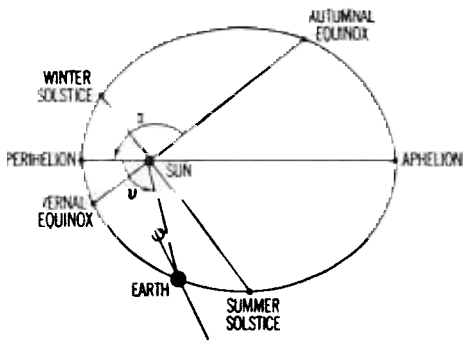
Schematic of the earth's orbit, showing the definition of the longitude of perihelion, Π.

tumnal equinox, measured in the direction of the earth's motion (Figure 1). At present, $\Pi = 102°$, so that perihelion occurs shortly after northern hemisphere winter solstice. The angle Π increases by $360°$ in approximately 20,000 years. A detailed description of the celestial mechanics involved may be found in the work of *Milankovitch* [1941]. Figure 2 shows how these orbital parameters have changed over the past 150,000 years, according to the recent calculation of *Berger* [1973].

If we let ν be the angle between lines connecting the sun with perihelion and with the location of the earth at time t (Figure 1), we have the relation (essentially Kepler's second law)

$$r^2 \frac{d\nu}{dt} = a^2(1 - \epsilon^2)^{1/2}$$

where

$$r(t) = a(1 - \epsilon^2)/\{1 + \epsilon \cos [\nu(t)]\}$$

is the earth-sun distance. (We have chosen the unit of time to be (1 year)$/2\pi$.) Defining $\omega = \nu + \Pi$ for fixed Π, we have

$$dt = \frac{r^2 d\omega}{a^2(1 - \epsilon^2)^{1/2}}$$

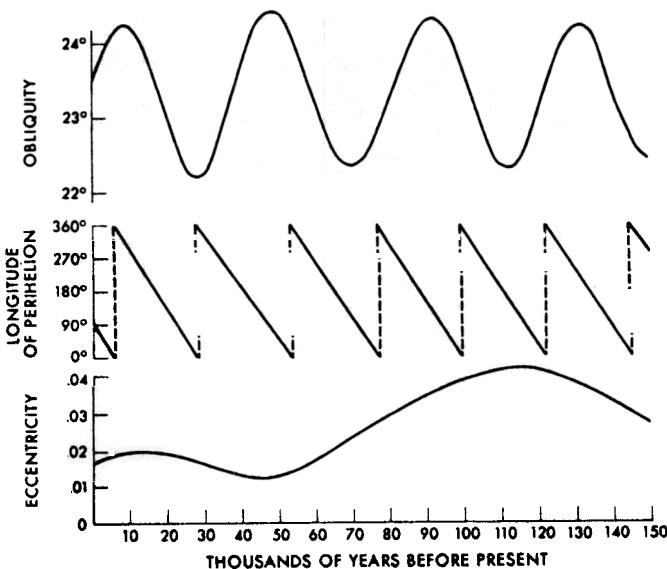The incident solar flux at the top of the atmosphere at time t and latitude θ is

$$S(t, \theta; \Phi, \epsilon, \Pi) = \frac{S_c a^2}{4r^2} \bar{S}[\omega(t; \epsilon, \Pi), \theta; \Phi]$$

where $(S_c/4)\bar{S}(\omega, \theta; \Phi)$ is the incident flux for a circular orbit, where $r = a$ and $\omega = t$, and $S_c/4$ is the global mean flux for this circular orbit. We refer to S_c as the solar constant and have

$$\frac{1}{2}\int_{-\pi/2}^{\pi/2} \bar{S}(\omega, \theta; \Phi) \cos (\theta) \, d\theta = 1$$

The function $\bar{S}(\omega, \theta; \Phi = 23.5°)$, evaluated from the formula by *Sellers* [1965], is plotted in Figure 3.

The annual mean flux at a given latitude for an eccentric orbit is

$$\frac{S_c}{4}\int_0^{2\pi} \bar{S}\frac{a^2}{r^2} \, dt = \frac{S_c}{4(1 - \epsilon^2)^{1/2}} \int_0^{2\pi} \bar{S} \, d\omega$$

The annual global mean is therefore proportional to $(1 - \epsilon^2)^{-1/2}$ but is independent of Φ and Π. The annual mean at any latitude, in addition to this weak dependence on ϵ, is dependent on Φ but once again independent of Π. The value of Π affects only the distribution of insolation around the year at any given latitude.

If we define $A \equiv (1$-planetary albedo), then the annual mean absorption at a given latitude is

$$\frac{S_c}{4}\int_0^{2\pi} \bar{S}A \frac{a^2}{r^2} \, dt = \frac{S_c}{4(1 - \epsilon^2)^{1/2}} \int_0^{2\pi} \bar{S}A \, d\omega \qquad (1)$$

If we alter Π, holding ϵ and Φ fixed, the absorbed solar radiation will change only if the planetary albedo changes as a function of ω. In order to study climatic responses to the perihelion cycle, we evidently need a model that predicts seasonally varying albedos as well as temperatures, given the seasonally varying insolation.

The insolation for an eccentric orbit has the following important symmetry:

$$S(\omega, \theta; \Phi, \epsilon, \Pi) = S(\omega + 180°, -\theta; \Phi, \epsilon, \Pi + 180°) \qquad (2)$$

The existence of this symmetry has often been referred to in arguments against the astronomical theory (see, for example, *Humphreys* [1940]), since the paleoclimatic record does not exhibit this symmetry; there seems to be no tendency for ice
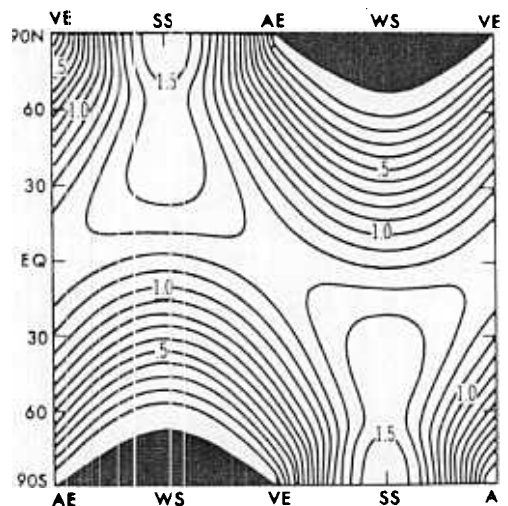

Fig. 2. The earth's orbital parameters for the last 150,000 years, according to *Berger* [1973].

Fig. 3. Insolation at the top of the atmosphere normalized by its annual global mean for a circular orbit and an obliquity of $23.5°$.

ages in one hemisphere to follow ice ages in the opposite hemisphere by 10,000 years. However, only models which are themselves symmetric with respect to the equator will preserve this symmetry in their climatic responses. The earth is not symmetric with respect to the equator. The southern hemisphere has less land than the northern hemisphere and smaller seasonal variations of temperature and albedo; it should therefore be relatively insensitive to any redistribution of insolation around the year, i.e., to the value of Π. A model designed to evaluate the astronomical theory must take into account this asymmetric continental distribution.

We illustrate the character and magnitude of the resulting perturbations in solar flux at the top of the atmosphere in Figures 4a and b. Figure 4a is the difference in the normalized flux $S(\omega, \theta)/(S_c/4)$ between 10,000 and 30,000 years B.P. (before present). Because of a low value of the eccentricity during this period, the difference is predominantly due to the change in obliquity. Figure 4b is the difference in insolation between 75,000 and 85,000 years B.P.; during this period, both changes in obliquity and longitude of the perihelion are important. Note that we have plotted the differences in insolation at the same values of ω, not the same values of t. If we choose time as the abscissa, the form of the plot depends on which points on the two orbits we choose to identify with $t = 0$. Equation (1) suggests that when considering changes in Π, it is useful to look at the variables as functions of ω and θ rather than of t and θ, and we shall consistently use this representation in the following. We emphasize that at a given latitude and point on the orbit the perturbations are quite substantial. The anomaly near the pole at southern hemisphere summer solstice in Figure 4b, for example, is 22% of the annual global mean insolation. We note also that these anomalies have a rather complicated structure. Since the climatic system is itself rather complicated, the problem of computing the detailed responses to these perturbations promises to be with us for some time. It is hoped, however, that calculations with relatively simple models will be sufficient to establish the plausibility of the astronomical theory.

3. THE MODEL

With these considerations in mind we construct a zonally symmetric model of the earth's energy balance and study the

sensitivity of its seasonally varying equilibrium states. The moderation of the seasonal variation of temperatures through heat storage in the oceans is modeled by assuming that part of the earth's surface is covered with a 40-m-deep isothermal layer of water. The time required to bring these 40 m of water (and the sea ice within this layer) into equilibrium is the longest explicit time scale in the model. In most of the cases discussed below a satisfactory equilibrium is reached in 50-100 years. Orbital parameter variations are negligible on such time scales, so we need only consider the model's equilibrium responses to different sets of orbital parameters. Time scales associated with the large heat capacity of abyssal waters or with the growth and deformation of continental glaciers may significantly alter conclusions drawn from such equilibrium calculations, a point that must be kept in mind when comparing our results with the geologic record.

The model we have chosen differs from other energy balance climate models discussed in the literature in certain important respects. In most other models (those patterned after *Sellers* [1969] and *Budyko* [1969]) the outgoing radiation at the top of the atmosphere, the meridional energy transport, and the albedos are parameterized in terms of surface temperatures. We have instead attempted to separate the surface and atmospheric energy balances and predict atmospheric lapse rates. Lapse rates can be expected to change seasonally as well as in response to other changes in external forcing. Figure 5 shows the observed seasonal variation of the potential temperature difference between 500 and 1000 mbar in the northern hemisphere (data taken from *Oort and Rasmussen* [1971]). The largest seasonal changes occur in high latitudes, precisely the region where most of our interest will be focused. *Wetherald and Manabe* [1975] have performed experiments testing the sensitivity of a general circulation model (GCM) forced with annual mean insolation to the value of the solar constant and obtain large changes in the static stability of the lower half of the troposphere in high latitudes. As we shall see, the changes in lapse rate allowed by the present model are of considerable importance in determining the sensitivity of surface temperatures.

In addition, rather than assuming some simple dependence of infrared cooling rates on surface temperature, we use the results of detailed radiative transfer calculations. In this way
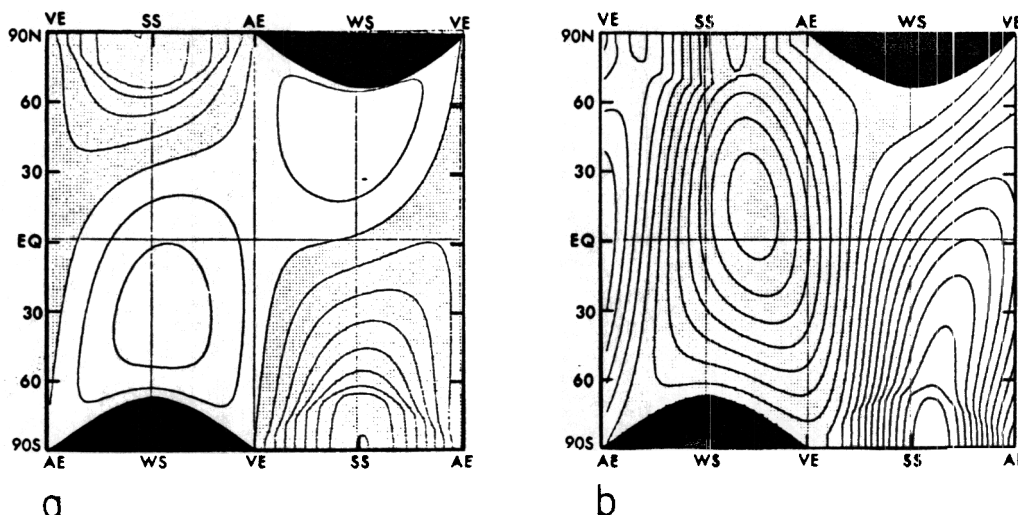

Fig. 4. (a) Difference in normalized insolation between 10,000 B.P. and 30,000 B.P. (b) Same difference between 75,000 B.P. and 85,000 B.P. The contour interval is 0.02 in both figures, and stippling indicates greater insolation at the earlier date.
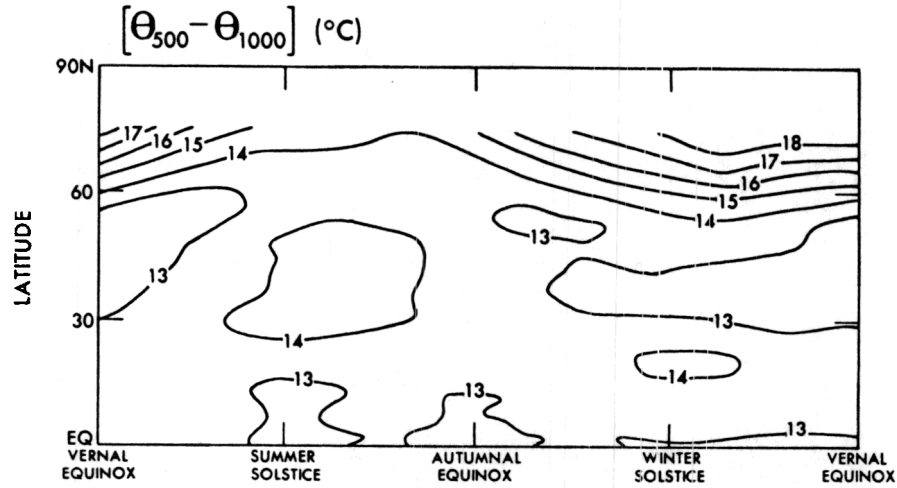
Fig. 5. Seasonal variation of the observed potential temperature difference between 500 and 1000 mbar in the northern hemisphere, taken from *Oort and Rasmussen* [1971].

we can make explicit assumptions regarding atmospheric absorbers and temperature profiles. We have, in particular, assumed that cloud amounts, heights, and radiative properties remain unchanged under the perturbations considered. We do not contend that cloud feedbacks of various sorts are of no importance for this problem. We feel, rather, that any attempt to incorporate them at this point is as likely to detract from as to improve our results. For the same reason we have ignored heat transport by ocean currents.

A detailed description of the model follows. The sensitivity of three versions of the model to the value of the solar constant is discussed in section 4, hoping to motivate our final choice of model for use in the orbital parameter study. The three versions differ in the assumed distribution of land and in the way in which land surface albedos are determined. The model's sensitivity to the different orbital parameters is discussed in section 5. In section 6 these results are combined to form the model's 'paleoclimatic record.'

The model consists of zonally averaged energy balances at two atmospheric levels. A linear diffusion simulates the meridional transport of energy by the atmosphere. We choose the potential temperatures at 250 and 750 mbar as our dependent variables:

$$\frac{\partial \Theta_k}{\partial t} = \frac{D}{r_e^2 \cos(\theta)} \frac{\partial}{\partial \theta} \left[\cos(\theta) \frac{\partial \Theta_k}{\partial \theta} \right] + \left(\frac{p_0}{p_k} \right)^\kappa \frac{Q_k}{c_a} \quad k = 1, 2 \quad (3)$$

The subscripts $k = 1, 2$ refer to variables defined at the upper and lower levels, respectively. Q is the diabatic heating; Θ is the potential temperature; p, θ, and t are pressure, latitude, and time; r_e is the radius of the earth; p_0 is the surface pressure; $\eta = (\gamma - 1)/\gamma$, where γ is the ratio of the heat capacity of air at constant pressure c_p to that at constant volume; and c_a is the heat capacity (per unit area) at constant pressure of half the atmospheric mass. The values of these and other parameters we shall require are listed in Table 1.

The diffusion coefficient D controls the meridional temperature gradients and therefore the strength of the albedo feedback [*Held and Suarez*, 1974]. We have used $D = 3.4 \times 10^6$ m²/s for all calculations reported below. This value is typical of the diffusivities used in other simple climate models and was

chosen to produce reasonable meridional temperature gradients. (D is incorrectly given as 1.7×10^6 m²/s in the work of *Suarez* [1976].) The distortions resulting from ignoring the possible dependence of eddy diffusivity on latitude, height, and horizontal and vertical potential temperature gradients, and of implicitly including all meridional energy transports in this diffusivity, are undoubtedly substantial. Perhaps the most significant distortion results from ignoring oceanic heat fluxes while forcing the atmosphere to produce reasonable meridional temperature gradients through the choice of diffusion coefficient.

At each latitude, two surface energy balance computations are performed, one over land and the other over ocean. Since the temperatures and albedos of the two surfaces can differ, radiative heating rates in the atmosphere are also computed separately over land and ocean. The results of these two computations are combined in a proportion determined by the fraction of the latitude circle assumed covered by land, $f(\theta)$, and added to (3), as illustrated in Figure 6.

Dividing the atmospheric heating rates Q_k into contributions due to long and short wave radiation, Q^{LW} and Q^{SW}, and to sensible and latent heat fluxes from the surface, Q^{SH} and Q^{LH},

$$Q_1 = (Q_1{}^{SW} + Q_1{}^{LW})_L f(\theta) + (Q_1{}^{SW} + Q_1{}^{LW})_0 [1 - f(\theta)] + Q^{CA}$$

$$Q_2 = (Q_2{}^{SW} + Q_2{}^{LW} + Q^{SH} + Q^{LH})_L f(\theta) + (Q_2{}^{SW} + Q_2{}^{LW} +$$

$$Q^{SH} + Q^{LH})_0 [1 - f(\theta)] - Q^{CA} \quad (4)$$

TABLE 1. Values of Parameters Used in This Study

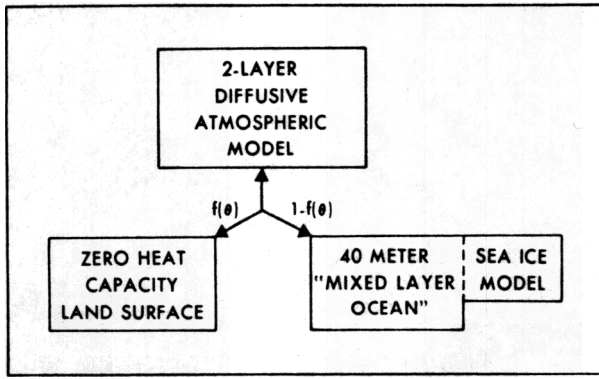| Parameter	Value
r_e, m	6.4×10^6
c_a, Ly deg⁻¹	122
p_0, mbar	1000
	2/7
σ, Ly deg⁻⁴ d⁻¹	1.17×10^{-7}
L, cal g⁻¹	595
L_f, cal g⁻¹	79.7
c_p, cal g⁻¹ deg⁻¹	0.24
ρ_i, g cm⁻³	
D, m² s⁻¹	3.4×10^6
c_0, cal cm⁻² deg⁻¹	4.0×10^3
C_D, g cm⁻² d⁻¹	52

Fig. 6. Schematic of the coupling between the model's atmosphere and the land and ocean surfaces; $f(\theta)$ is the fraction of land around a latitude circle.

where subscripts L and O refer to quantities computed over land and ocean, respectively. We assume that water vapor condenses at the same latitude at which it evaporates and in the lower half of the atmosphere, except when the convective adjustment transfers some of this heating into the upper layer (as described below).

Q^{SW} and Q^{LW} are computed by using the scheme described by *Held and Suarez* [1978].

Whenever the model's 'static stability,' $\Theta = (\Theta_1 - \Theta_2)/2$, falls below a critical temperature-dependent value, Θ_{crit}, an amount of energy Q^{CA} is exchanged between the two layers, leaving unchanged the mean atmospheric temperature, $\bar{T} = (T_1 + T_2)/2$, and forcing Θ to equal Θ_{crit}. We set $\Theta_{crit} = (\Theta_1^{MA} - \Theta_2^{MA})/2$, where Θ_1^{MA} and Θ_2^{MA} are the 250- and 750-mbar potential temperatures on that moist adiabat with mean temperature $\bar{T} = [(p_1/p_0)^\kappa \Theta_1^{MA} + (p_2/p_0)^\kappa \Theta_2^{MA}]/2$. Θ_{crit} as a function of $\bar{T}$ is shown in Figure 3 of *Held and Suarez* [1978].

The land is assumed to be a zero heat capacity surface where the following balance holds:

$$0 = (1 - \alpha_L)S + \mathcal{L} - \sigma T_{*L}^4 - Q_L^{SH} - Q_L^{LH}$$

where α_L is the land surface albedo, $\mathcal{L}$ is the downward longwave at the surface, and S is the incident shortwave flux at the ground obtained from the radiative calculation. Assuming a simple drag law at the surface, the sensible and latent heat fluxes are given by

$$Q_L^{SH} = C_D c_p (T_{*L} - T_a)$$

$$Q_L^{LH} = C_D L [R(T_{*L}) - 0.8R(T_a)]$$

T_a is the atmospheric temperature at the ground, L is the latent heat of vaporization, and C_D is a drag coefficient (see Table 1). $R(T)$ is the saturation mixing ratio at 1000 mbar. The surface is assumed to be saturated, while the relative humidity of the atmosphere at the ground is assumed to be 80%. The land surface temperature T_{*L} is obtained by satisfying this balance. The model's dependence on the scheme used to compute the albedos α_L will be discussed in section 4.

The 40-m-deep ocean is assumed isothermal in the vertical, with temperature T_{*O}. In the absence of sea ice the rate of change of T_{*O} is given by

$$c_O \frac{\partial T_{*O}}{\partial t} = (1 - \alpha_O)S_* + \mathcal{L} - \sigma T_{*O}^4 - Q_O^{SH} - Q_O^{LH} \qquad (5)$$

where $c_O = 4000$ Ly deg^{-1} and $\alpha_O = 0.1$. The computation of sensible and latent heat fluxes over ocean is identical to that

over land. When the temperature falls below 273°K, sea ice is formed and α_O is set equal to 0.7. The sea ice thickness I is then predicted by using a scheme similar to that used by *Bryan* [1969].

Energy is conserved by this model in the sense that

$$\frac{d}{dt} \int d\theta \cos \theta \{c_a(T_1 + T_2) + [1 - f(\theta)](c_O T_O + \rho_I L_f I)\}$$

equals the net downward radiative flux at the top of the atmosphere.

Equation (3) is integrated numerically by using a Crank-Nicholson scheme. The time step is (1 year)/100 and the meridional resolution 2° latitude. In some cases the sea ice thickness is still growing at the end of the integration, but the heat flux through the ice (which is inversely proportional to ice thickness) is then negligible in the atmosphere's energy balance.

This model is essentially the same as a two-level primitive equation atmospheric model designed by the authors for climatic sensitivity studies [*Held and Suarez*, 1978] except that all of the dynamics in that model have been replaced by a linear lateral diffusion of heat. We view this study, in part, as preparation for a similar study with the primitive equation model.

4. SENSITIVITY TO THE SOLAR CONSTANT

We describe the sensitivity of three different versions of this model to the value of the solar constant. In all three versions the earth's orbit is assumed to be circular, $\epsilon = 0$, and the obliquity is set equal to 23.5°.

In the first version the fraction of land, $f(\theta)$, is assumed to equal 0.3 at all latitudes, and the land albedo α_L is assumed to be the following discontinuous function of land surface temperature

$$\alpha_L = 0.1 \qquad T_{*L} > 273°K$$
$$\alpha_L = 0.7 \qquad T_{*L} < 273°K \qquad (6)$$

In the second version, $f(\theta)$ is still taken to be 0.3 everywhere, but a snow budget is included in the calculation by making a very simple assumption regarding the rate of snowfall. Land albedos are then assumed to depend on the presence ($\alpha_L = 0.7$) or absence ($\alpha_L = 0.1$) of snow.

In the third version we retain this snow budget but choose $f(\theta)$ to correspond to the present continental distribution.

Version 1: Temperature-Dependent Albedo

The results of experiments at several values of the solar constant with $f(\theta) = 0.3$ and with land surface albedos given by (6) are summarized in Figures 7 and 8.

Figure 7 is a plot of the solar constant dependence of the seasonal maximum and minimum 'snow cover' and sea ice extents. (Land is considered 'snow covered' when $T_{*L} < 273°K$). Below a solar constant of 1.96 Ly/min the only possible equilibrium state of the model is the totally snow- and ice-covered state. For solar constants greater than 1.96 Ly/min, two states are possible: the totally ice covered state and the partially ice covered state shown in the figure. The totally ice covered state is an equilibrium state for all solar constants less than 2.6 Ly/min.

As one might surmise from the unrealistically high values of the solar constant in Figure 7, the model has a high planetary albedo (~0.33 when the surface albedo is 0.1). As we are primarily concerned with qualitative differences between equilibrium states, we have not adjusted the radiation model to
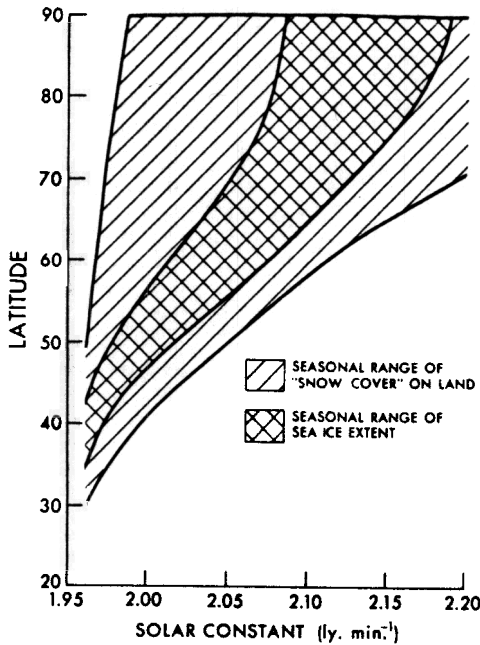
Fig. 7. Behavior of the 'snow cover' and sea ice limits in version 1 as a function of solar constant.

correct this bias (an adjustment which could most plausibly be made by modifying our cloud amounts or albedos).

A noteworthy feature in Figure 7 is the extreme sensitivity of permanent snow cover over land, which exists for a range of less than 1% of the solar constant. As was discussed by *Held and Suarez* [1974] for an annual mean climate model, the sensitivity of the snow line and the strength of the albedo feedback are inversely proportional to the temperature gradient near the snow line. In this seasonally varying case the sensitivity of permanent snow cover, the snow cover which survives the summer, is controlled by the small land surface temperature gradients during summer. Once summer surface temperatures at high latitudes fall below freezing, they do so over a large area. The weaker sensitivity of the maximum snow cover may be similarly explained by noting its dependence on larger mid-latitude surface temperature gradients during winter. The moderate seasonal variation of the sea ice leads to an ice extent intermediate in sensitivity between these two extremes. (The model produces a very large area of sea ice, presumably because we have neglected oceanic heat transport.)

The sensitivity of the model's surface temperatures is strongly latitude dependent. Annual mean surface temperatures averaged over land and ocean are plotted in Figure 8 for three values of S_c along with annual mean '500-mbar' potential temperatures, $\bar{\Theta} \equiv (\Theta_1 + \Theta_2)/2$, and annual mean potential temperature differences between the two model layers, $\Theta_1 - \Theta_2$. Surface temperatures are much more sensitive in high than in low latitudes, while the sensitivity of 500-mbar temperatures is nearly independent of latitude, a difference accounted for by changes in the model's static stability. The simplest diffusive energy balance models [*North*, 1975] do not predict such strong latitudinal dependence in sensitivity. The results from the GCM calculations of *Wetherald and Manabe* [1975], however, are qualitatively similar to those obtained here.

The balance of terms contributing to the rate of change of the model's stability $\partial\theta/\partial t$ is strongly latitude dependent. In low latitudes the primary balance is between destabilization

due to surface fluxes and stabilization by moist convective adjustment. Θ is therefore maintained at its moist adiabatic value Θ_{crit}. Since Θ_{crit} increases with increasing temperature, tropical surface temperatures are less sensitive than 500-mbar temperatures (as suggested by *Kraus* [1973]).

In high latitudes the balance is between the stabilizing effect of the radiative fluxes (the infrared cooling rate of the lower half of the atmosphere being much greater than that of the upper half) and destabilization by lateral heat transport (the poleward diffusive flux being larger in the lower layer, where the temperature gradient is larger). We find a very similar high-latitude stability balance in our companion two-level primitive equation model [*Held and Suarez*, 1978]. As temperatures increase in high latitudes, destabilization by surface fluxes increases, partly due to albedo changes, and stabilities
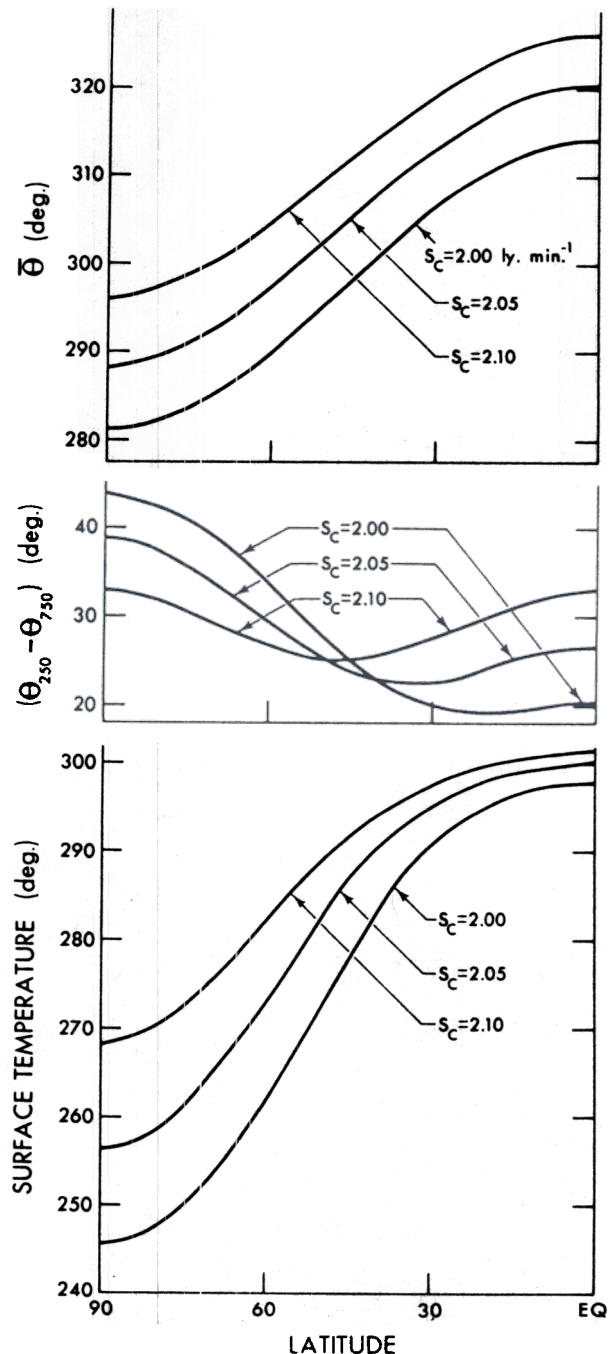

Fig. 8. Meridional distributions of temperatures and static stabilities produced by version 1 of the model.

decrease until compensating changes in longwave cooling and transport are generated.

In the earth's atmosphere we expect the vertical transport of sensible heat by large-scale eddies to play a significant stabilizing role in mid-latitudes. We have ignored this transport completely. We find that the model's differential horizontal transport is capable of maintaining reasonable mid-latitude stabilities, and rather than introduce additional model parameters by trying to incorporate the vertical sensible heat flux, we have simply decided to omit it. How this distortion of the stability balance affects climatic sensitivity is unclear. (*Schneider and Dickinson* [1974] suggest that this vertical flux has a significant destabilizing effect.)

Figure 9 shows the seasonal variation of the potential temperature difference between 500 mbar and the ground $(\Theta - T_s)$ predicted by the model for $S_c = 2.05$ Ly/min, to be compared with the observations in Figure 5. There is qualitative agreement between model and observations. Both, for example, show a relative maximum in the mid-latitude stability during summer, which in the model is due to moist convection forcing $\Theta = \Theta_{crit}$ at these times.

Although this model climate does seem reasonable in some respects, of prime concern for the ice age problem is the sensitivity of the perennial snow cover over land, i.e., continental glaciers. As we have seen in Figure 7, perennial snow cover appears at solar contants only slightly greater than the critical value below which the ice-covered earth is the only equilibrium state. We try to obtain a more reasonable result for this part of the model before proceeding.

Version 2: Inclusion of a Snow Budget

This exaggerated sensitivity of the perennial snow cover is largely due to the dependence of land surface albedos on land surface temperatures. Surface albedos over land should depend on the presence of snow, albedos remaining high until the snow accumulated in winter has melted. Unfortunately, without having a model which predicts water vapor transport, the effects of snow accumulation can only be studied by making some more or less arbitrary assumption regarding the rate of snowfall. We simply assume that snow falls at a fixed latitude-

dependent rate whenever temperatures fall below freezing. The snow depth is then predicted as described by *Suarez* [1976].

We now let land surface albedos depend on the presence of snow:

$$\alpha_L = 0.1 \qquad S_L = 0$$

$$\alpha_L = 0.7 \qquad S_L > 0$$

Equilibrium states are again obtained at several values of the solar constant, and the maximum and minimum snow and sea ice covers are plotted in Figure 10. Compared with version 1, the sensitivity of the minimum snow extent is sharply reduced, with 'continental glaciation' occurring between the solar constants of 1.96 and 2.06 Ly/min. The maximum snow limit is not significantly affected by the snow budget.

The sensitivity of the model's perennial snow cover is evidently strongly dependent on the treatment of the snow budget. Our assumption of a prescribed snow fall rate seems to yield more plausible results than those obtained with a temperature-dependent albedo, so we retain this snow budget in the calculations described below.

Version 3: The Continental Distribution

We now choose $f(\theta)$ corresponding to the actual continental distribution. The snow and sea ice limits produced by this version of the model are shown in Figure 11. Perennial snow cover occurs in the model's northern hemisphere for a range of 3% of the solar constant, a smaller range than that obtained with version 2 because of the large seasonal variation in high northern latitudes. Perennial snow cover is present in the southern hemisphere for a range of nearly 5% of the solar constant and disappears from the Antarctic continent discontinuously as S_c is increased.

The behavior of the hemispheric mean surface temperatures as a function of solar constant (Figure 12) is worth noting. The southern hemisphere is colder at solar constants below the transition from an ice-covered to an ice-free Antarctic continent and warmer at solar constants above this point. Evidently, a larger seasonal variation can have either a warming or a cooling effect, depending on the value of S_c. At a value
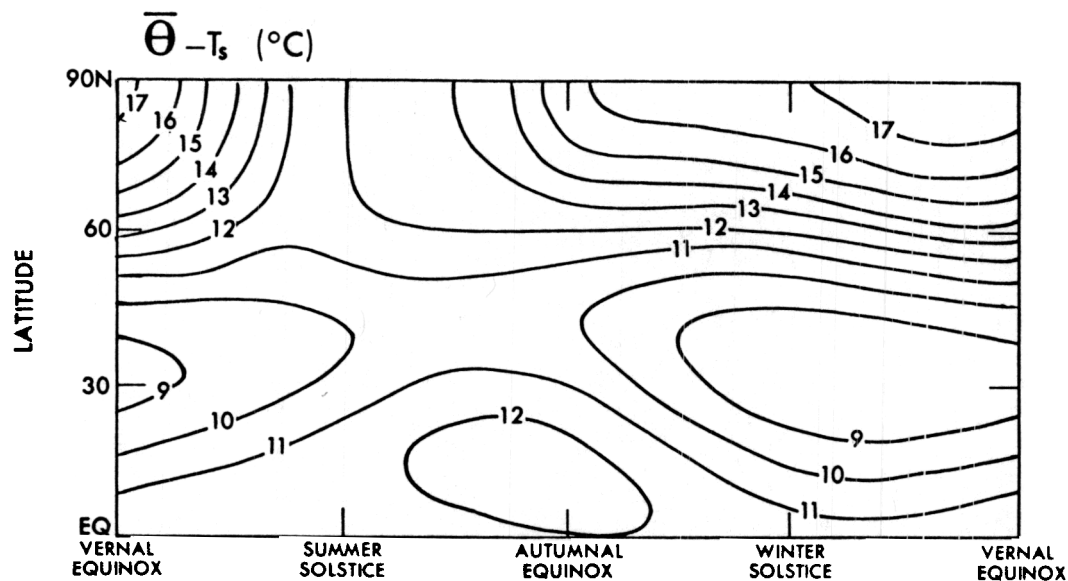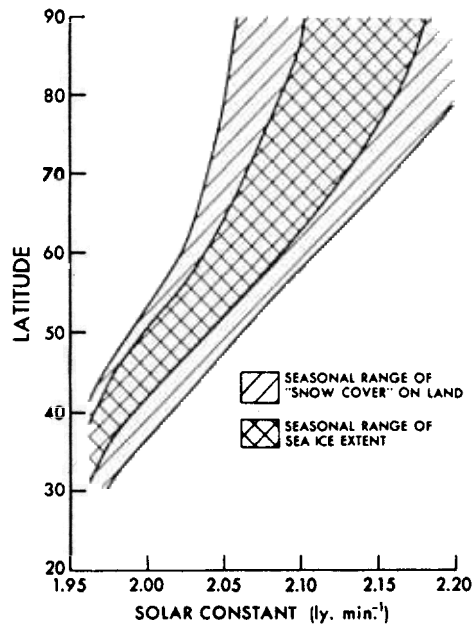

Fig. 9. Seasonal variation of the static stability in the lower half of the model atmosphere $(\Theta = (\Theta_1 + \Theta_3)/2$, and T_s is the atmospheric temperature extrapolated to 1000 mbar) for version 1 with $S_c = 2.05$ Ly min^{-1}.

Behavior of snow cover and sea ice limits in version 2 as a function of solar constant.

Fig. 12. Hemispheric mean surface temperatures for version 3.

5. SENSITIVITY TO THE ORBITAL PARAMETERS

We describe orbital parameter sensitivity experiments with version 3 of the model, and with the solar constant fixed at S_c = 2.01 Ly/min. If we choose a higher value of solar constant, we find that the Antarctic ice cap disappears for some values of the orbital parameters. As it is well established that the Antarctic ice cap has existed throughout the Pleistocene [Flint, 1971], we choose a solar constant small enough that our model agrees with the record in this respect. S_c = 2.01 produces a rather cold climate with an annual global mean surface temperature of ~9°C when ϵ = 0 and Φ = 23.5°. Albedo feedback is very strong about this point, the sensitivity of global mean temperature to a 1% change in solar constant being ~4°C (as compared with 1°C in the absence of albedo feedback).

We begin by considering the response to obliquity variations in the range 22° $\leq \Phi \leq$ 25°, retaining a circular orbit. The anomaly in insolation for a 1.5° obliquity increase is shown in Figure 13, along with the unperturbed (Φ = 23.5°) sea ice and snow boundaries. Figure 14 shows the response to obliquity variations of the seasonal limits of snow and sea ice in the northern hemisphere. The northern hemisphere's permanent snow line over land once again is particularly sensitive, retreating from 61°N to 79° N as Φ is increased from 22° to 25°. The boundary of the permanent sea ice also retreats significantly,

of S_c low enough that there is significant sea ice and snow cover when the seasonal variation is small, a larger seasonal variation will likely have a warming effect, since snow will melt in the summer, decreasing annual mean albedos. The GCM of *Wetherald and Manabe* [1972] behaves in just this way. At a solar constant large enough that little ice or snow is present when the seasonal variation is small, an increased seasonal variation will have a cooling effect, since snowfall in the winter will increase the annual mean albedos. The southern hemisphere's seasonal variation is small, so its mean temperature changes from colder to warmer than that of the northern hemisphere when its permanent ice and snow disappear. In our orbital parameter experiments we will be working with a solar constant sufficiently low that we expect a larger seasonal variation (large obliquity or perihelion near summer solstice) to produce a warmer climate.
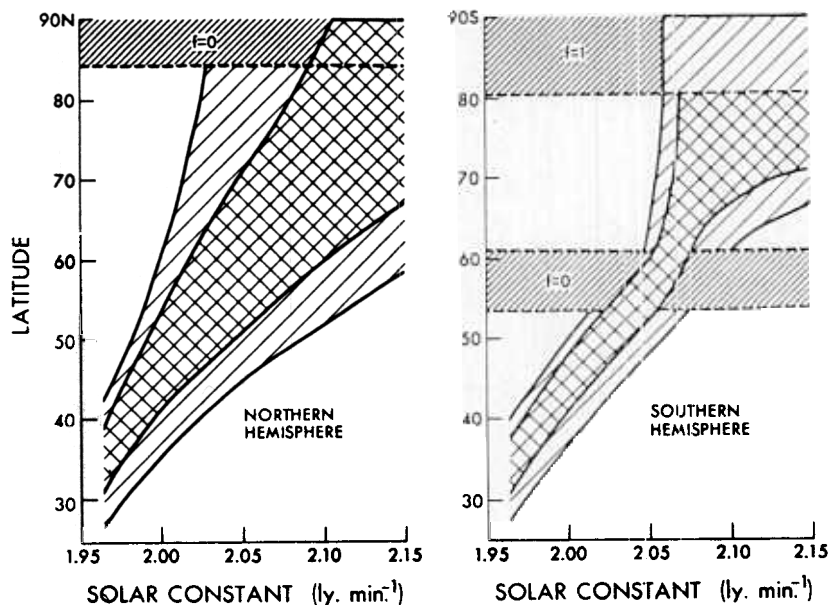
Fig. 11. Behavior of snow cover and sea ice limits in the two hemispheres of version 3 as a function of solar constant.
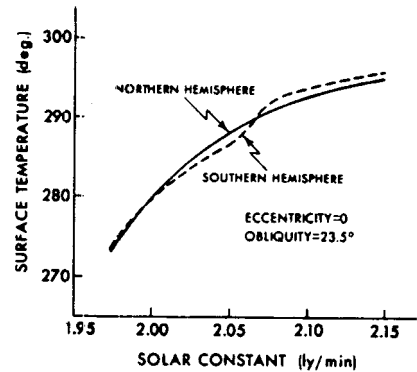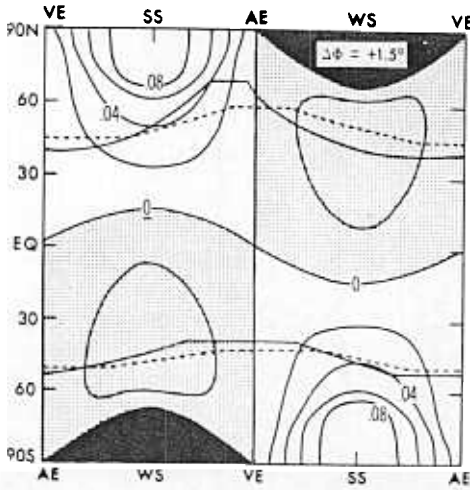
Fig. 13. Anomaly in normalized insolation due to a 1.5° increase in obliquity, together with the snow (solid lines) and sea ice (dashed lines) boundaries produced in the unperturbed case (Φ = 23.5°) by version 3.
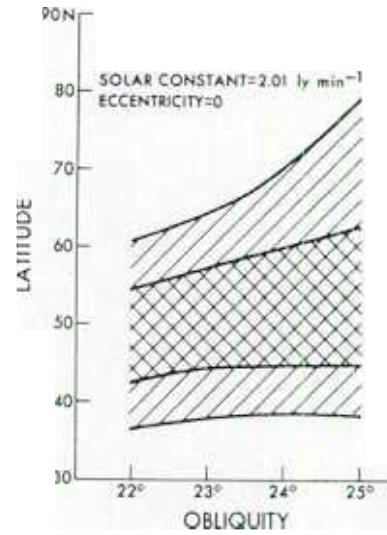

Fig. 14. Behavior of snow cover and sea ice limits in the northern hemisphere of version 3 as a function of the obliquity.

but there is little movement of the maximum snow and sea ice limits.

Figure 15 shows the northern hemisphere temperature changes at the surface and at 500 mbar produced by the 3° obliquity increase. North of 30°, surface temperatures are substantially more sensitive than 500-mbar temperatures; once again changes in static stability are substantial. The hemispheric mean surface temperature change is 1.9°C.

The same change in perennial snow cover (61°–79°N) can be accomplished by increasing the solar constant from 2.0 to 2.025 Ly min^{-1}, approximately 1.3%. The temperature response to such an increase in solar constant is 5°C in the hemispheric mean and >9°C in high northern latitudes, as shown in the lower half of Figure 15. The fact that the solar constant change requires a larger change in annual mean high-latitude temperatures to produce the same displacement of the perennial snow line emphasizes the importance of the seasonal redistribution of insolation resulting from the obliquity perturbation.

Movement of the sea ice and snow boundaries in the southern hemisphere in response to obliquity variations is negligible ($\leq 2°$ latitude equals one grid point). Referring to Figure 13, we note that the sea ice and snow boundaries have little seasonal variation and are located at a latitude where the annual mean insolation anomaly due to obliquity variation is small. If the ice cap boundary were poleward of ~60° latitude, however, we would expect substantial reponse to the annual mean obliquity anomaly, as illustrated in Figure 10 of *Held and Suarez* [1974].

The value of the eccentricity ϵ affects the insolation in two distinct ways: by modifying the annual global mean insolation by the factor $(1 - \epsilon^2)^{-1/2}$ and by determining the amplitude of the seasonal redistribution of insolation due to changes in the longitude of perihelion. The insolation anomalies for (ϵ = 0.04, Π = 0°) and (ϵ = 0.04, Π= 90°), with ϵ = 0 as reference, are shown in Figure 16 along with the unperturbed snow and sea ice boundaries. The anomalies for Π = 180° and Π = 270° can be obtained from the symmetry (2).

For ϵ = 0.04 the $(1 - \epsilon^2)^{-1/2}$ factor is equivalent to a change in solar constant of 0.08%. From our solar constant experiments we estimate the response to be ~0.3°C in northern hemisphere mean surface temperature and ~1° latitude in the

northern hemisphere's perennial snow line. The perturbation in snow line is more than an order of magnitude smaller than that obtained from the obliquity variation; the perturbation in hemispheric mean temperature is somewhat less than an order of magnitude smaller.

The redistribution of insolation, however, is an $o(\epsilon)$ rather than an $o(\epsilon^2)$ effect. Experiments were performed with ϵ = 0.04, Φ = 23.5°, and with 10 values of Π. The right half of Figure 17 is a plot of the resulting maximum and minimum snow cover and sea ice extents in the northern hemisphere. In the left half of Figure 17 we have plotted the mean northern hemisphere surface temperature along with the curve
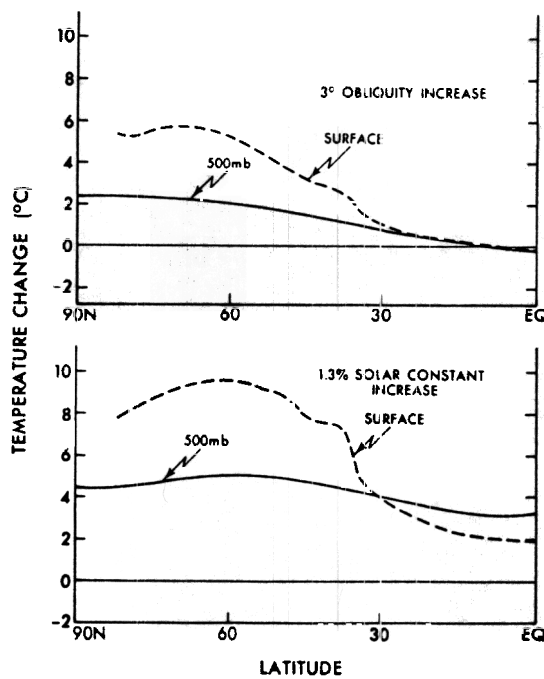
$$283 + 0.8 \cos (\Pi - 240)$$

Fig. 15. Temperature changes produced by a 3° increase in obliquity and those produced by a solar constant increase that results in the same meridional displacement of the perennial snow cover limit.
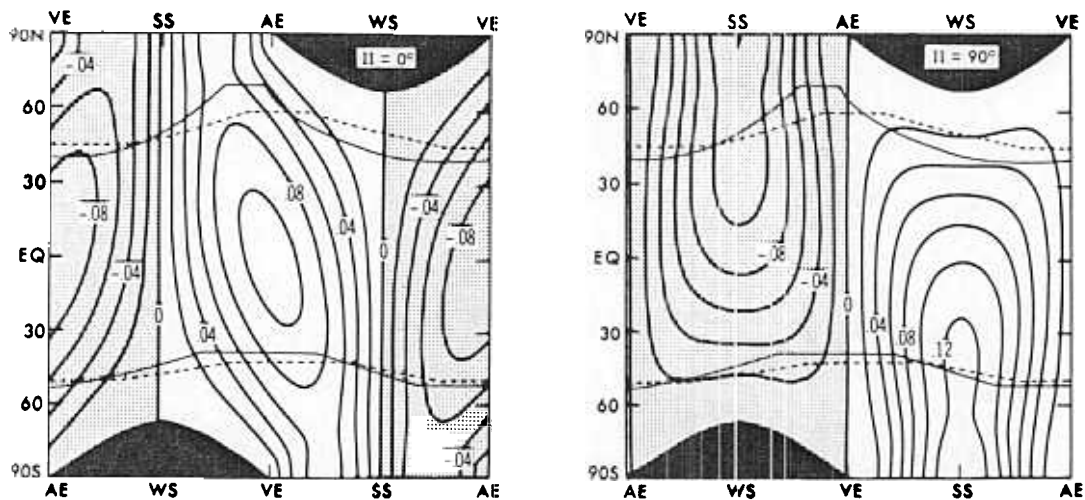
Fig. 16. Anomaly in normalized insolation at two values of Π and ε = 0.04, with ε = 0 as reference. Also shown, the snow (solid lines) and sea ice (dashed lines) boundaries produced with ε = 0 by version 3.

This curve provides a reasonable fit except for the Π = 45° case. (Evidently, 2° meridional grid resolution is inadequate for resolving the small shifts in the maximum snow and sea ice limits. These small shifts have a significant effect on the hemispheric mean temperature response.) We see from Figure 17 that the model's response to the perihelion cycle with ε = 0.04 is comparable in magnitude to its response to obliquity variations of ±1.5°.

Values of Π = 0 and Π = 180° produce snow and ice boundaries similar to those of the ε = 0 case. Perihelion is at the equinoxes in these cases, and the biggest insolation anomalies occur when polar latitudes are receiving little insolation. For Π = 90° and Π = 270°, perihelion is at one of the solstices, and the anomalies bear more directly on the sea ice and snow margins. The warmest case is Π = 270°, the sign of the temperature response being that of the insolation anomaly during the summer half year, as suggested by *Milankovitch* [1941]. Insolation is large and surface temperature gradients are small during the summer, and therefore summer insolation anomalies produce large changes in albedos that in turn cause large changes in absorption.

In going from Π = 90° to Π = 270° we find that the mean northern hemisphere albedo decreases by 0.01. Averaged over the hemisphere, we find that 20% of the decrease is due to increased absorption in the atmosphere, 20% at the ocean surface, and 60% at the land surface. In addition, only half of

the change in absorption at the land surface occurs at those latitudes that become 'deglaciated,' the rest occurring at latitudes that are snow covered for only part of the year in both experiments. Thus if one considers only the changes in albedo due to the glaciers themselves, one underestimates the global mean change in planetary albedo by a factor of 3.

Changes in the model's southern hemisphere in response to the perihelion cycle are very small (≤ 0.3°C in hemispheric mean temperature), too small to be accurately determined with our meridional resolution. The changes that do occur generally have the same sign as those in the northern hemisphere. In any case, the symmetry (2) is definitely not observed in the model's responses.

6. The Model's Paleoclimatic Record

Experiments have been performed with the orbital parameters displayed in Figure 2 at each 5000-year interval into the past. The results for the variations in snow and sea ice extent, presented previously by *Suarez and Held* [1976], are shown in Figure 18 along with one of the most detailed records of paleotemperatures in the North Atlantic [*Sancetta et al.*, 1973]. The corresponding changes in mean northern hemisphere surface temperature, δ{T}, are plotted in the lower half of Figure 19. Assuming that the responses to the several orbital parameters are additive, we extract from the results of the preceding section the formula
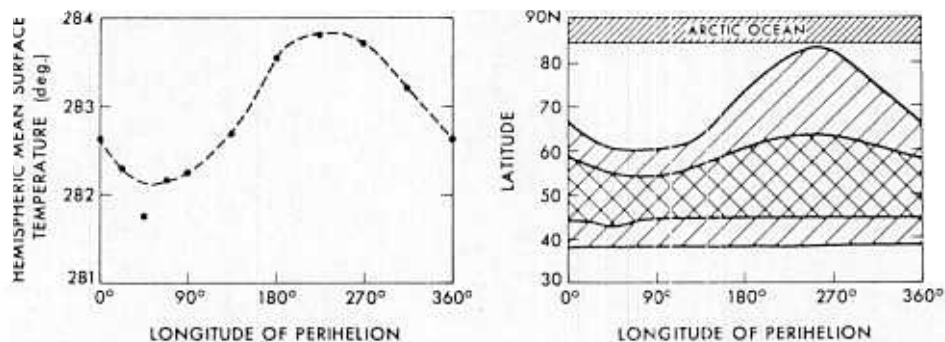

Fig. 17. Northern hemispheric mean surface temperature and snow and sea ice limits as a function of the longitude of perihelion with ε = 0.04.

$$\delta\{T\} = 0.62\delta\Phi + \left(\frac{\epsilon}{0.04}\right) 0.8 \cos(\pi - 240) + \left(\frac{\epsilon}{0.04}\right)^2 0.32 \tag{7}$$

where $\delta\{T\}$ is in degrees Celsius and $\delta\Phi$ is in degrees.

The three separate contributions are plotted in the upper part of Figure 19; their sum is the solid line in the lower half of the figure. We see that the response of $\{T\}$, at least, is reasonably linear. (Some of the differences between this approximation and the actual model results may, in fact, be due to insufficient meridional resolution.) The fact that nonlinearities are small eliminates the possibility of explaining the strong 100,000-year period found in spectral analyses of paleoclimatic records [*Hays et al.*, 1976].

There is an obvious discrepancy between the model's paleoclimatic record and the actual record: the model predicts that the earth is presently in the midst of an ice age. Temperatures predicted for the present are colder than those predicted for 18,000 B.P., the time of the last glacial maximum. Agreement with the record, at least for the last 30,000 years, would be improved if the model's responses were shifted toward the present by 5000 or 6000 years. At least three plausible explanations exist for this discrepancy:

1. The time required to change the temperature of abyssal waters, or to build and destroy continental glaciers, could produce a lag between the record and model results that assumes the system responds instantaneously to the forcing.
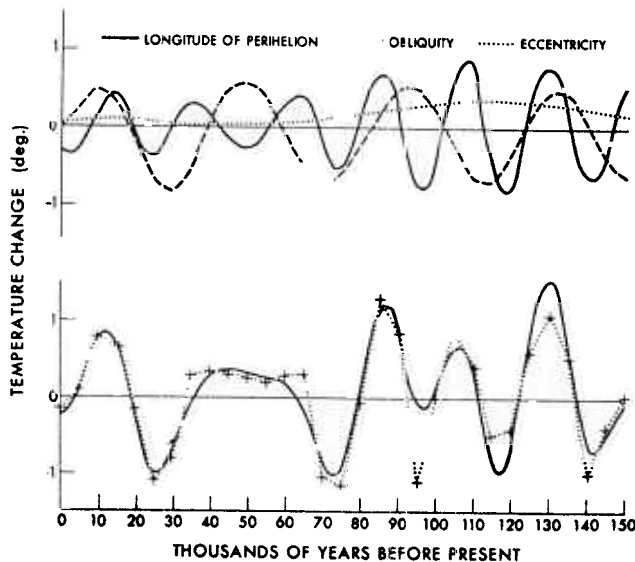

Fig. 19. (Bottom) Changes in northern hemispheric mean surface temperature for the experiments shown in the lower half of Figure 18, together with temperature changes given by (7). (Top) The three terms in the right-hand side of (7).

2. Other sources of variability exist on these time scales. If the earth's climate is indeed as sensitive as that of the model described here, it would be surprising if natural variability or the response to varying volcanic aerosol loading of the stratosphere were not observed in the record.

3. Our model may simply be distorting the true equilibrium response to the orbital parameter variations. Because of the many uncertainties in these calculations—most notably the neglect of the oceanic heat transport, the neglect of variations in cloudiness, the assumption of linear diffusive transport in the atmosphere, and the arbitrarily prescribed snowfall rate—we may expect some distortion. However, inspection of Figure 2 shows that the present values of the orbital parameters are very similar to their values at 18,000 B.P. So it seems highly unlikely that climatic differences between 18,000 B.P. and the present can be explained in terms of an equilibrium response of the sort discussed here. Nevertheless, obtaining a better estimate than that presented here of the climate's equilibrium response to orbital parameter changes remains an important problem, and one we believe more tractable than those presented by the first two possibilities.

7. CONCLUSIONS

In a preliminary attempt to demonstrate the plausibility of the astronomical theory of the ice ages, we have evaluated the responses of a diffusive energy balance climate model to orbital parameter variations. The responses obtained are comparable in magnitude to those produced by a 1% change in solar constant. Albedo changes, variations in static stability, the details of the snow budget, and the asymmetric continental distribution all seem to play significant roles in determining the character of these responses. The qualitative similarity between the model's paleoclimatic record and the actual record for the past 150,000 years suggests that a significant fraction of the variance on these time scales is due to orbital variations.

The model's continental glaciers and temperatures in high northern latitudes are exceptionally sensitive, not only to orbital variations, but also to variations in the solar constant. It
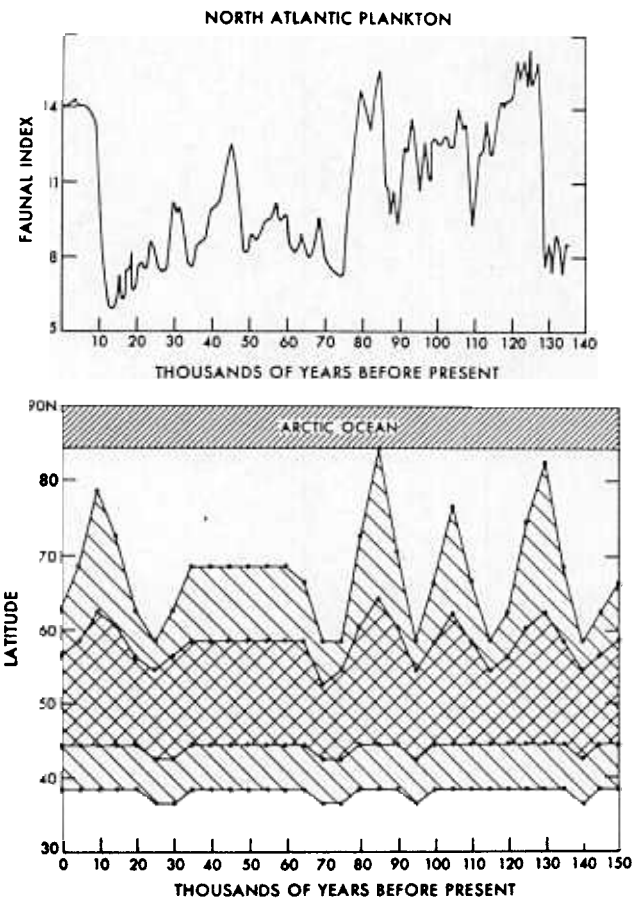
Fig. 18. (Bottom) Response of the model's snow and sea ice limits to the orbital parameter variations of the last 150,000 years. (Top) Paleotemperatures inferred from planktonic foraminifera in a North Atlantic deep-sea core, taken from *Sancetta et al.* [1973].

is certainly possible that our model is exaggerating this sensitivity. We note, for example, that the assumed difference between bare soil or open water (0.1) and snow or sea ice (0.7) surface albedos is undoubtedly too large, particularly with regard to seasonal snow cover. But are not the ice ages, in fact, evidence for such exceptional sensitivity? Is it possible for the orbital variations to produce climatic responses of ice age proportions without high northern latitudes being particularly sensitive to all sorts of small perturbations in the earth's energy balance? Calculations with more convincing climate models are certainly needed to answer these questions.

References

Berger, A. L., *Théorie Astronomique des Paléoclimats,* 197 pp., Université de Louvain, Louvain, Belgium, 1973.

Bryan, K., Climate and the ocean circulation, III, *Mon. Weather Rev.,* 97, 806–827, 1969.

Budyko, M. I., The effect of solar constant variation on the climate of the earth, *Tellus, 21,* 611–619, 1969.

Flint, R. F., *Glacial and Quaternary Geology,* 892 pp., John Wiley, New York, 1971.

Hays, J. D., J. Imbrie, and N. J. Shackelton, Variations of the earth's orbit: Pacemaker of the ice ages, *Science, 194,* 1121–1132, 1976.

Held, I. M., and M. J. Suarez, Simple albedo feedback models of the icecaps, *Tellus, 26,* 613–629, 1974.

Held, I. M., and M. J. Suarez, A two-level primitive equation atmospheric model designed for climatic sensitivity experiments, *J. Atmos. Sci., 35,* 206–229, 1978.

Humphreys, W. J., *Physcis of the Air,* 676 pp., McGraw-Hill, New York, 1940.

Kraus, E. B., Comparison between ice age and present general circulations, *Nature, 245,* 129–133, 1973.

McIntyre, A., et al., The surface of the ice-age earth, *Science, 191,* 1131–1137, 1976.

Milankovitch, M., *Canon of Insolation and the Ice Age Problem,* 482 pp., Royal Serbian Academy, Belgrade, 1941. (Translation, Israel Program for Scientific Translation, Jerusalem, 1969.)

North, G. R., Analytical solution to a simple climate model with diffusive heat transport, *J. Atmos. Sci., 32,* 1301–1307, 1975.

Oort, A., and E. M. Rasmussen, Atmospheric circulation statistics, *Prof. Pap. 5,* Nat. Oceanic and Atmos. Admin., Washington, D. C., 1971.

Sancetta, C., J. Imbrie, and N. G. Kipp, Climatic record of the past 130,000 years in North Atlantic deep-sea core V23-82: Correlation with the terrestrial record, *Quarternary Res., 3,* 110–116, 1973.

Schneider, S. H., and R. E. Dickinson, Climate modeling, *Rev. Geophys. Space Phys., 12,* 447–493, 1974.

Sellers, W. D., *Physical Climatology,* 212 pp., The University of Chicago Press, Chicago, Ill., 1965.

Sellers, W. D., A global climate model based on the energy balance of the earth-atmosphere system, *J. Appl. Meteorol., 8,* 392–400, 1969.

Suarez, M. J., An evaluation of the astronomical theory of the ice ages, Ph.D. thesis, Princeton Univ., Princeton, N. J., 1976.

Suarez, M. J., and I. M. Held, Modelling climatic response to orbital parameter variations, *Nature, 263,* 46–47, 1976.

Wetherald, R. T., and S. Manabe, Response of the joint ocean-atmosphere model to the seasonal variation of the solar radiation, *Mon. Weather Rev., 100,* 42–59, 1972.

Wetherald, R. T., and S. Manabe, The effects of changing the solar constant on the climate of a general circulation model, *J. Atmos. Sci., 29,* 870–876, 1975.